Infectious Disease Modelling 9 (2024) 204–213

Contents lists available at ScienceDirect

Infectious Disease Modelling

journal homepage: www.keaipublishing.com/idm

Structural network characteristics affect epidemic severity and prediction in social contact networks

Jae McKee [a, b], Tad Dallas [c, *]

[a] Bioinnovation Program, Tulane University, New Orleans, LA, 70118, USA
[b] Department of Medicine, Tulane University School of Medicine, New Orleans, LA, 70112, USA
[c] Department of Biological Sciences, University of South Carolina, Columbia, SC, 29208, USA

ARTICLE INFO

Article history:
Received 29 August 2023
Received in revised form 14 November 2023
Accepted 27 December 2023
Available online 28 December 2023
Handling Editor: Dr Yiming Shao

Keywords:
Social contact network
Spectral radius
Epidemic severity
Basic reproduction number

ABSTRACT

Understanding and mitigating epidemic spread in complex networks requires the measurement of structural network properties associated with epidemic risk. Classic measures of epidemic thresholds like the basic reproduction number (R_0) have been adapted to account for the structure of social contact networks but still may be unable to capture epidemic potential relative to more recent measures based on spectral graph properties. Here, we explore the ability of R_0 and the spectral radius of the social contact network to estimate epidemic susceptibility. To do so, we simulate epidemics on a series of constructed (small world, scale-free, and random networks) and a collection of over 700 empirical biological social contact networks. Further, we explore how other network properties are related to these two epidemic estimators (R_0 and spectral radius) and mean infection prevalence in simulated epidemics. Overall, we find that network properties strongly influence epidemic dynamics and the subsequent utility of R_0 and spectral radius as indicators of epidemic risk.

1. Introduction

Epidemics can have devastating global effects on human and wildlife populations (World Health Organization, 2019). The development of epidemic management strategies is difficult, and the control of disease continues to be a complex and multifaceted challenge (Jeger, 2004; Wearing et al., 2005). The combination of epidemiology and network theory is one approach that addresses this challenge (Danon et al., 2011; Keeling & Eames, 2005; Pastor-Satorras et al., 2015). Social contact networks can be used to represent pathogen transmission pathways between individuals, allowing the application of epidemiological theory to model epidemic progression. Combining these two fields can inform management decisions through the improved understanding of both population structure and disease dynamics (Craft, 2015; Kiskowski & Chowell, 2016; Silk et al., 2017). Specifically, understanding how the structure of these social contact networks which increase epidemic risk may help inform network-based intervention and mitigation strategies.

* Corresponding author.
E-mail address: tad.a.dallas@gmail.com (T. Dallas).
Peer review under responsibility of KeAi Communications Co., Ltd.

https://doi.org/10.1016/j.idm.2023.12.008

Perhaps the most widely used metric for evaluating the likelihood of an epidemic outbreak on a network is the basic reproduction number (R_0), which is the number of individuals that one infected individual would infect in a completely susceptible population (Dietz, 1993). Hence, R_0 can be used to predict pathogen invasion potential, which is the likelihood that a pathogen can persist within a susceptible population. There are various methods to calculate R_0 (Heffernan et al., 2005), such as the survival function (Heesterbeek & Dietz, 1996), which considers vaccination strategy, and the next generation method (Diekmann et al., 1990), which relies on the next-generation matrix. Many studies have emphasized the importance of R_0 in strategic planning of outbreak control for a number of diseases, including Ebola (Van Kerkhove et al., 2015), malaria (Griffin, 2015; Smith et al., 2007), dengue (Rodrigues et al., 2016; Supriatna, 2009), and measles (Guerra et al., 2017). It is commonly assumed that if R_0 is less than one, the pathogen will not invade, and if R_0 is greater than one, the pathogen will invade. However, some research has challenged this ideology, arguing that some pathogens can persist when R_0 is less than one and vice versa (Li et al., 2011). Regardless, a larger R_0 should also typically correspond to a larger epidemic, suggesting that R_0 also may capture aspects of epidemic size or severity (but see (Holme & Masuda, 2015)).

While R_0 is the most commonly used measure of epidemic potential, it is based on models which assume a well-mixed population (i.e., everyone interacts with everyone). Extensions of classic R_0 estimation to social contact networks has provided a nice link between classic epidemiological theory and transmission networks (Trapman et al., 2016; Herrera et al., 2016), but current measures of R_0 only consider some combination of the mean and variance in degree (the number of connections each node has in the contact network). These approaches recognize that heterogeneity in connections among individuals can influence the resulting pathogen emergence potential, but argue that these first two moments of the degree distribution capture the necessary information of network structure to epidemic emergence. However, considering the range of configurations that social contact networks can take, this approach may be insufficient at estimating pathogen invasion potential and/or epidemic susceptibility in networked systems.

Other recently developed epidemic risk estimators based on spectral properties of social contact networks provide promising novel ways to estimate epidemic risk (Sarkar & Jalan, 2018). Spectral properties refer to the characteristics of the eigenvalues of the matrices associated with a given network. Many of these measures use the adjacency matrix – which describes the potential transmission pathways among susceptible individuals – to estimate the potential for a pathogen to invade and cause an epidemic (Goltsev et al., 2012; Wang et al., 2003). Spectral properties of the adjacency matrix often reveal important qualities of their corresponding network (Sarkar & Jalan, 2018).

One particularly useful spectral characteristic is spectral radius. Similar to R_0, spectral radius has been suggested as an estimator of pathogen invasion potential given the social contact network throughout which the disease may propagate (Ganesh et al., 2005). The spectral radius of a network is the largest eigenvalue of its adjacency matrix. Because the largest eigenvalue is directly related to network topology, the spectral radius is thought to correspond to the overall connectivity of the network, which was illustrated in one study that decreased spectral radius by removing links (Van Mieghem et al., 2011). Hence, the lower the spectral radius, the lower the connectivity, and the lower the invasion potential (between different networks subjected to the same pathogen). Using this logic, prior studies have attempted to lower spectral radius in order to reduce epidemic spread (Saha et al., 2015). Although less common than R_0, spectral radius has been used in recent research as an important measure for the analysis of real world networks relating to the spread of diseases, including hepatitis B (Suleman & Riaz, 2017). In addition, one classic metric of network susceptibility to epidemic spread is the N-Intertwined Mean-Field Approximation (NIMFA) epidemic threshold, which is inversely proportional to spectral radius. Hence, through the incorporation of NIMFA, some studies have indirectly relied on spectral radius as an indicator of epidemic spread potential (Liu & Van Mieghem, 2016, 2018; Socievole et al., 2016).

The multiple ways that pathogen invasion potential can be estimated (e.g., R_0, spectral radius, etc.) could lead to confusion over when to trust one method over the other in public health scenarios. A shortcoming of the spectral radius is that it only considers information on the social contact network, ignoring important pathogen-specific parameters like transmission and recovery rates. However, while estimates of R_0 for networks do incorporate these parameters, they may oversimplify the influence of the complex connections between individuals by only considering the first two moments of the degree distribution. Many different network structures could have those two moments, and could lead to drastically different epidemic outcomes. This represents a clear knowledge gap, as estimating epidemic risk from these network-based approaches can lead to general insights into how to design networks, as well as which individuals to target for testing or treatment during the course of the epidemic. Using a large set of constructed and empirical social contact networks, we explored the sensitivity of our two measures of pathogen invasion potential (spectral radius and R_0) to epidemic severity estimates obtained through simulated epidemics. We further explore how aspects of the network was constructed (e.g., scale-free graph) and graph properties (e.g., modularity) influenced resulting epidemic dynamics. Together, we provide evidence that the spectral radius is able to capture pathogen invasion potential well in simulated and empirical networks, highlight the role that social contact network structure plays in epidemic emergence, and suggest clear next steps in utilizing network-based epidemic emergence estimators.

2. Methods

2.1. Constructed and empirical networks

We considered three types of constructed networks for this study: scale-free, random, and small-world. We constructed and ran simulations on 100 networks from each of these network types.

Scale-free networks were constructed using the Barabasi-Albert graph generation algorithm (Barabási & Albert, 1999). Scale-free networks are characterized by a power law decay of the cumulative distribution (Barabási & Bonabeau, 2003). Intuitively, this means that network characteristics are unaffected by network size. In other words, if a scale-free network grows, its fundamental structure remains the same. Many real networks have been found to exhibit scale-free properties, such as human sexual contact networks (Liljeros et al., 2001), bird social networks (Small et al., 2007), and primate social networks (Akbaş et al., 2015). Barabasi-Albert networks are formed by preferential attachment. At each timestep, a node and some number (m) of links are added; these links form preferentially with high degree nodes (Barabási & Albert, 1999). To explore the effect of network size and preferential attachment on pathogen invasion and infection dynamics, we created 100 networks, each with a random number of nodes in the network (between 10 and 1000) and a random preferential attachment (ω) value (between 0.00 and 3.00). The number of links added per timestep, m, was held consistent at $m = 1$ for all networks to keep link density consistent throughout the networks.

Random networks were constructed according to the Erdos-Renyi model (Erdös & Rényi, 1959). Random networks are characterized by links between nodes forming according to a uniform probability distribution. Although random networks are often regarded as imperfect models of biological systems (Newman et al., 2003), they have been used to model social contact in many studies on epidemic invasion (Eames & Keeling, 2003; Huerta & Tsimring, 2002; Keeling, 1999). To explore the effect of network size and link density on pathogen invasion and infection dynamics, we created 100 networks, each with a random number of nodes (n) between 10 and 1000 and a random number of links per node (k) between 1.00 and 4.00. These parameters (n and k) were then multiplied together to obtain the total number of links within the network and then connected to nodes at random. Self-loops were not allowed. Only fully-connected networks were considered. If a non-fully-connected network was formed, the largest component was extracted. If the largest component was less than 10 nodes in size, then both n and k were redrawn at random, and the process was repeated until a fully-connected network between 10 and 1000 nodes was obtained.

Small-world networks were constructed according to the Watts-Strogatz random link-rewiring procedure (Watts & Strogatz, 1998). Small-world networks are characterized by their incorporation of both qualities of lattice networks, in which links are distributed uniformly between nodes, as well as qualities of random networks. Many real networks are considered to have small world properties, including transportation networks (Latora & Marchiori, 2002; Li & Cai, 2004; Sen et al., 2003), human social contact networks (Milgram, 1967; Salathé et al., 2010), and animal social contact networks, such as lions (Craft et al., 2011). To explore the effect of network size and long-range connections on pathogen invasion and infection dynamics, we created 100 networks, each with a random number of nodes (n) between 10 and 1000 and a random percentage of links rerouted (p) between 0.00 and 1.00. Dimension (d) and neighborhood (n_e) were both set at 1 to keep link density consistent throughout the networks. Self-loops were not allowed, and only fully-connected networks were considered. If a non-fully-connected network was formed, the largest component was extracted. If the largest component was less than 10 nodes in size, then n and p were redrawn at random, and the process was repeated until a fully-connected network between 10 and 1000 nodes was obtained.

We also considered empirical social contact networks: 782 total networks collected from studies of bird (39), fish (16), insect (272), mammal (401), and reptile (54) populations, compiled by (Sah et al., 2019). These social contact networks ranged in size between 4 and 1100 individuals, and varied in the number and organization of interactions among these individuals substantially.

2.2. Structural network characteristics

We examined four structural characteristics of constructed and empirical social contact networks: modularity, degree variance, mean degree, and link density. Modularity measures the extent to which a network is divided into subgroups and is particularly useful in ecology for community detection (Grilli et al., 2016). Modularity was estimated as Barber's Q (Barber, 2007). Node degree is defined as the number of contacts a given node has, and the resulting degree distribution is incredibly useful in characterizing network structure (Kossinets & Watts, 2006), especially for applications of understanding pathogen emergence in contact networks (Castellano & Pastor-Satorras, 2019). We explore the first two moments of the degree distribution; the mean degree and the degree variance. Finally, we considered the influence of link density, defined as the percentage of potential links that are realized.

2.3. Epidemic risk estimators

We considered two different measures of social contact networks that have been used in various studies to assess pathogen outbreak and epidemic severity: basic reproduction number (Herrera et al., 2016; Volz & Meyers, 2009) and spectral radius (Valdano et al., 2015; Youssef & Scoglio, 2011). First, we calculated a network form of R_0, which attempts to estimate

pathogen invasion potential. In a social contact network, we define R_0 as a function of the distribution of links in the network (Equation (1)).

$$R_0 = T \times \left(\langle k \rangle - 1 + \frac{\sigma_{\langle k \rangle}}{\langle k \rangle} \right) \tag{1}$$

where $T = \frac{\beta}{\beta+\gamma}$, $\langle k \rangle$ is the mean of the degree distribution, and $\sigma_{\langle k \rangle}$ is the standard deviation of the degree distribution. The degree of a node is the number of links that are connected to it. The degree distribution of a network is the probability distribution of the degrees of all of the nodes within the network. In the expression for T, β is the transmission probability and γ is the recovery rate. This calculation for R_0 is reproduced from a previous derivation of R_0 given a social contact network (Britton, 2019; Campbell & Salathé, 2013). Unlike the traditional calculation for R_0, it is important to note that because this is a network measure, it is not based off of a well-mixed population assumption.

A second measure of social contact networks related to pathogen outbreak potential is spectral radius (ζ). This is quantified as the dominant eigenvalue of the adjacency matrix, describing the links between nodes in the network (Equation (2) and Fig. 1b).

$$\zeta = max\{|\lambda_1|, \ldots, |\lambda_n|\} \tag{2}$$

where $\lambda_1 \ldots, \lambda_n$ are the eigenvalues of the adjacency matrix. Spectral radius was standardized by the square root of the total links in the network, so as to make networks of different sizes comparable.

2.4. Simulating epidemics

Epidemics were simulated using a Susceptible-Infected-Recovered (*SIR*) model on each simulated and empirical network (Fig. 1c). Epidemics were initialized by infecting one randomly-selected node and allowing the epidemic to progress over timesteps ($t = 50$), with each timestep equivalent to one day. This model assumes that every node in a population is either susceptible to (S), infected with (I), or recovered from (R) pathogen infection. Links between nodes represent infection pathways. Nodes connected to infected nodes become infected with some transmission probability ($\beta = 0.1$), and infected nodes become uninfected based on a recovery probability ($\gamma = 0.05$). Infection is a stochastic process, meaning that each node connected to an infected node becomes infected each day with probability β, and infected nodes recover with probability γ. Nodes connected to multiple infected nodes are assumed to become infected through two independent trials (i.e., there is no multiplicative infection risk). Nodes that recover from infection are presumed to be immune for the remainder of the simulation. Both infection and recovery were modeled with a binomial distribution ($S \Rightarrow I$: $B(t, \beta)$ and $I \Rightarrow R$: $B(t, \gamma)$ respectfully).

As measures of epidemics on these networks, we calculated the fraction of individuals infected through the course of the epidemic (i.e., infection prevalence). This process of pathogen propagation was repeated 100 times for each network, starting from a random node every time. We averaged the results of each 100 trials to provide a mean epidemic size and mean infection prevalence for each network. We included all trials in these calculations, even those with no infection propagation. All correlation coefficients were calculated as Pearson correlation coefficients.

3. Results

3.1. Network structure and epidemic severity across network types

Structural properties of the networks (e.g., modularity) varied across constructed network types (Fig. S1) and influenced resulting epidemic dynamics in our simulations (Fig. 2). All network types displayed a strong negative relationship between modularity and mean infection prevalence, reinforcing previous links between modularity, nestedness, and spectral radius in complex networks (Stevanovic, 2014). All network types also displayed a strong positive effect of mean degree and degree variance on mean infection prevalence. The effect of link density differed between network types (Fig. 2). The strength of correlations also varied over property ranges, specifically for scale-free networks. For example, there was a stronger negative correlation between modularity and mean infection prevalence in scale-free networks with larger modularity values (i.e. modularity greater than 0.5) compared to the correlation among scale-free networks with smaller modularity values. Additionally, there was a stronger positive correlation between mean degree and mean infection prevalence in scale-free networks with smaller mean degree values (i.e. mean degree less than 250) compared to the correlation among scale-free networks with larger mean degree values.

3.2. The influence of static network properties on epidemic susceptibility indicators and its relationship with epidemic severity

We found that structural network characteristics have varied influence on epidemic susceptibility indicators (spectral radius and R_0) depending on network type (Figs. S2 and S3). All network types displayed a strong positive influence between spectral radius and degree centralization (Fig. S2). However, the impact of modularity, assortativity, degree variance, mean

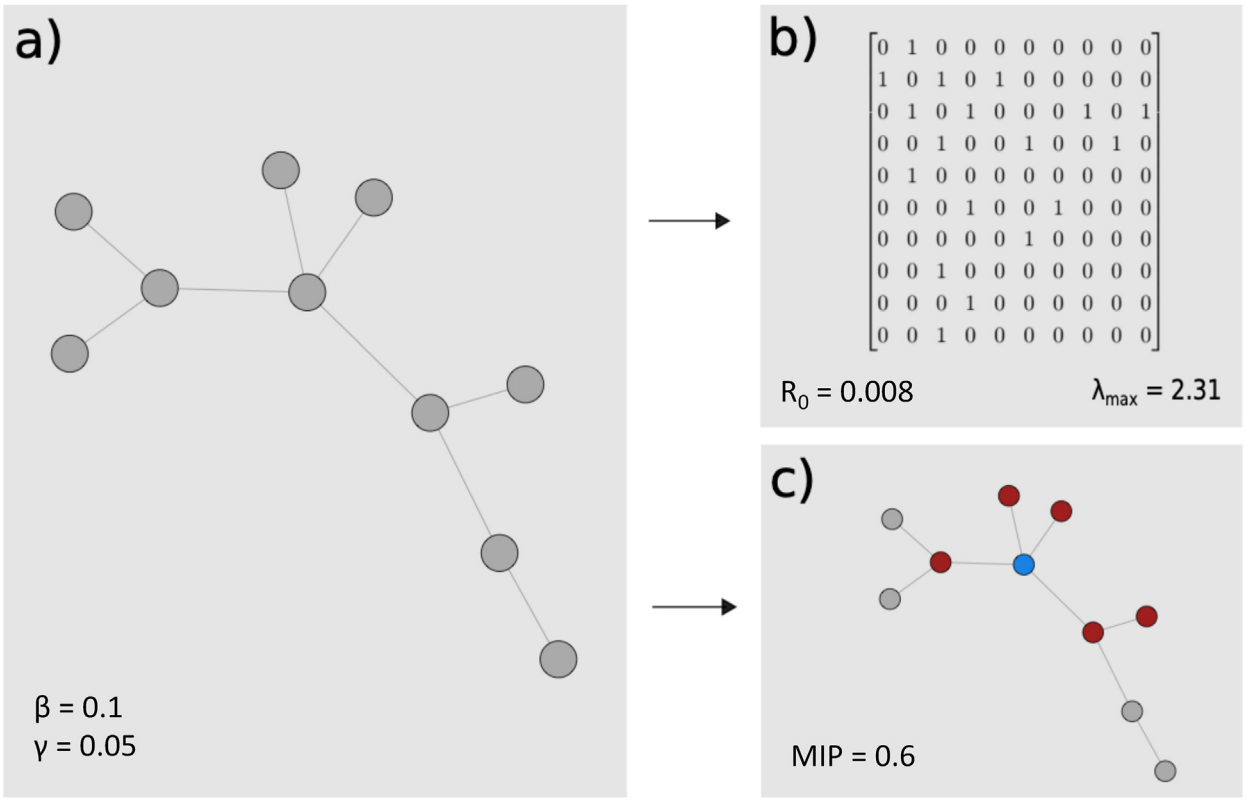

Fig. 1. Conceptual diagram illustrating the link between the representation of a network as a graph (*a*) and an adjacency matrix (*b*). By simulating epidemics across this network, we can draw connections between network structure, spectral radius (λ_{max}), R_0 and potential for disease outbreak. SIR model simulations across the network resulted in the infection of susceptible nodes with transmission probability ($\beta = 0.1$) and recovery probability ($\gamma = 0.05$) (*c*; grey is susceptible, red is infected, and blue is recovered).

degree, transitivity, link density, and network size on spectral radius varied across network types (see Supplemental Materials). For basic reproduction number (R_0), all network types displayed a strong positive relationship between degree variance and R_0 as well as between mean degree and R_0. None of the network types displayed a significant relationship between network size and R_0. The effect of modularity, assortativity, degree centralization, transitivity, and link density on R_0 was not consistent across network types (Fig. S3).

We also looked at the relationship between both epidemic susceptibility indicators and epidemic severity (Fig. 4). All network types displayed a positive relationship between R_0 and mean infection prevalence (Fig. 3), though the effects were often non-linear, and a sharp threshold was observed in the empirical networks that limits the utility of R_0 as a potential indicator of epidemic severity. A similar trend was observed using an alternative calculation of the basic reproduction number that excludes both infection probability and recovery probability (Fig. S4). The relationship between spectral radius and the basic reproduction number was not consistent across network types; scale-free, small world, and real networks displayed strong positive relationships, while random networks did not display a significant relationship. This suggests that network type and corresponding structural properties of networks may influence the reliability of epidemic susceptibility indicators.

4. Discussion

The distribution of links in complex networks influences the potential for epidemic spread. Here, we explored the ability of estimators of epidemic susceptibility (spectral radius and R_0) to capture epidemic size in a series of constructed and empirical networks. By constructing networks to adhere to different topologies (scale-free, random, and small world), and simulating epidemics across these networks, we provide general support of epidemic susceptibility estimators to capture potential epidemic susceptibility across a wide range of networks. Our findings add to a large body of work on the exploration of network topology as it relates to epidemic outcome. We found highest mean infection prevalence in our random and real networks. In contrast, a previous study that simulated pathogen spread through a variety of constructed networks found scale-free networks allowed for the largest epidemic spread compared to random, lattice, and small-world networks (Shirely & Rushton, 2005). This discrepancy highlights the importance of taking into account topological properties beyond network

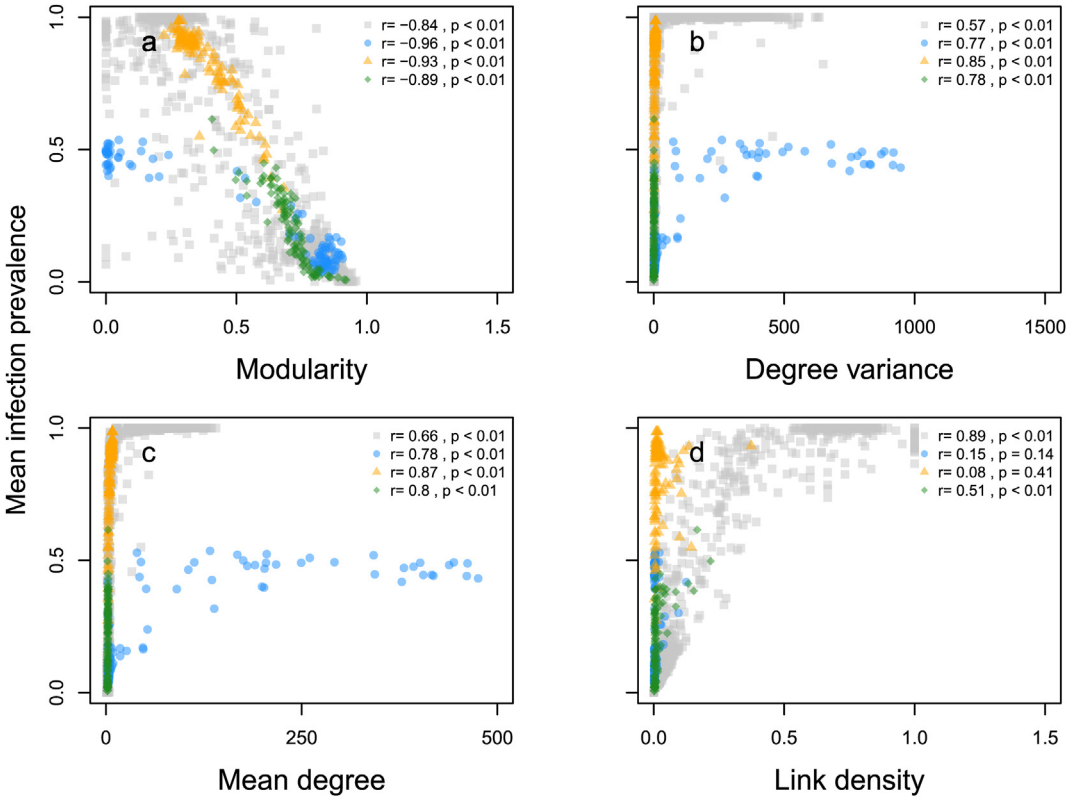

Fig. 2. The effect of various network properties on epidemic severity for both real and constructed networks. Each scatter plot point represents a different network with colors corresponding to network type. Grey points correspond to real networks, blue points correspond to scale-free networks, orange points correspond to random networks, and green points correspond to small-world networks. The graphs display the effect of modularity (*a*), degree variance (*b*), mean degree (*c*), and link density (*d*) on mean infection prevalence, which was calculated from averaging the result of 100 SIR simulations per network. The legends indicate correlation coefficients between each network property and mean infection prevalence (r) for each network type.

type. Due to variation in both method of construction and choice of construction parameters, networks that are categorically similar in type, may differ greatly in epidemic susceptibility.

The different network types varied greatly in their structural properties (e.g., modularity), which had a clear influence on the epidemic outcomes in simulations on both constructed and empirical networks. The stronger negative correlation between infection prevalence and modularity observed among scale-free networks with higher modularity is consistent with previous studies on scale-free networks, which have suggested modularity as a measure to quantify strength of community structure (Dinh & Thai, 2013). Our results indicate a potential threshold of modularity (or community strength) needed to observe a relationship between modularity and infection prevalence in scale-free networks. A similar threshold effect might explain the reason for the weakening correlation between infection prevalence and mean degree among scale-free networks with larger mean degree values. Mean degree is linked to both network size and connectivity. Perhaps a threshold exists for scale-free networks in which increasing network connectivity no longer increases epidemic spread. Understanding the relationships between various network properties can allow us to construct secure networks that are not vulnerable to pathogen spread as well as choose indicators that can best evaluate epidemic likelihood in existing networks.

Network structure varied as a function of network type, and this variation in structural properties of the network had a pronounced influence on estimators of epidemic susceptibility – spectral radius and basic reproduction number R_0. These two measures were, often non-linearly, related to epidemic severity in simulated epidemics across both constructed and empirical networks, and differed in their utility across network types. For instance, R_0 was more clearly related to mean infection prevalence for random networks, but had a weaker switch-like relationship in the empirical social networks. This finding was consistent with a recent study that found the basic reproduction number did not accurately capture the epidemic dynamics of simulated pathogen spread through empirical contact networks that were representative of subsets of Italian and Dutch populations (Liu et al., 2018). Together, this suggests that both spectral radius and R_0 may be useful indicators of potential epidemic severity, but that such forecasts recognize the variation in the relationship. Future estimators of epidemic severity may benefit from incorporating information on other aspects of network structure, as we found other aspects of network structure to be associated with infection prevalence (e.g., modularity and link density). This supports previous findings that networks with lower link density had a lower risk of epidemic spread, as explored for HIV (Tatem et al., 2012)

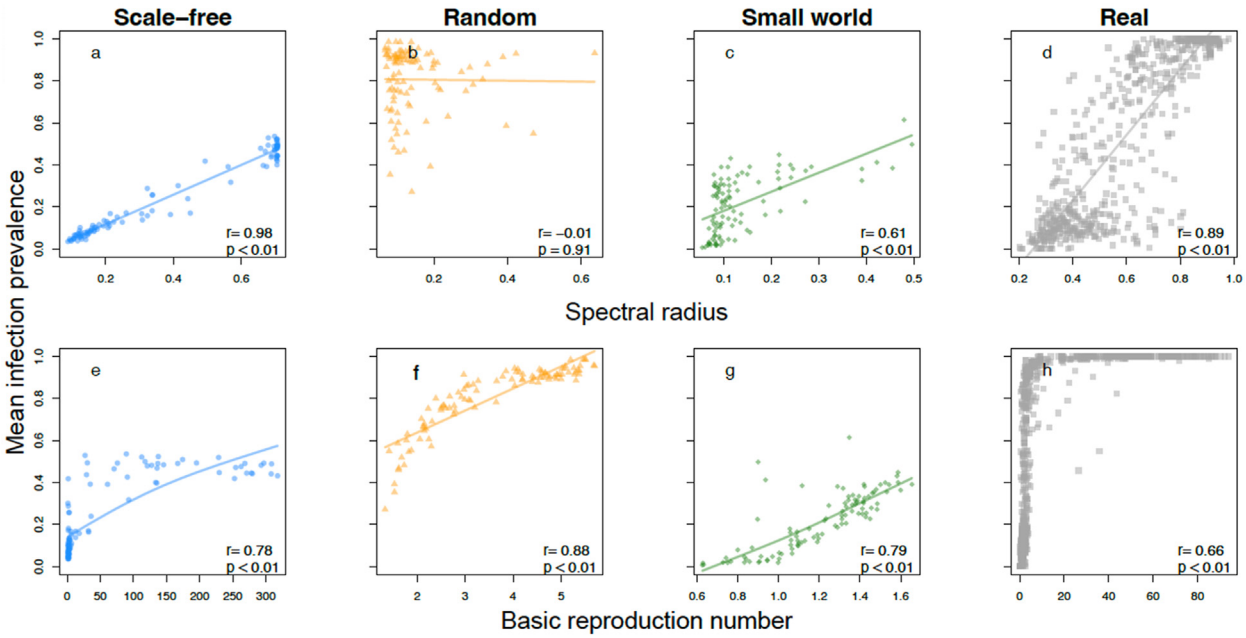

Fig. 3. The relationship between epidemic susceptibility indicators and epidemic severity. Each scatter plot point represents a different network with colors corresponding to network type. The graphs display the relationship between spectral radius and mean infection prevalence for scale-free (*a*), random (*b*), small world (*c*), and real (*d*) networks as well as the relationship between basic reproduction number and mean infection prevalence for scale-free (*e*), random (*f*), small world (*g*), and real (*h*) networks. Mean infection prevalence was calculated from averaging the result of 100 SIR simulations per network. The legends indicate correlation coefficients between each network property and mean infection prevalence (r) for each network type.

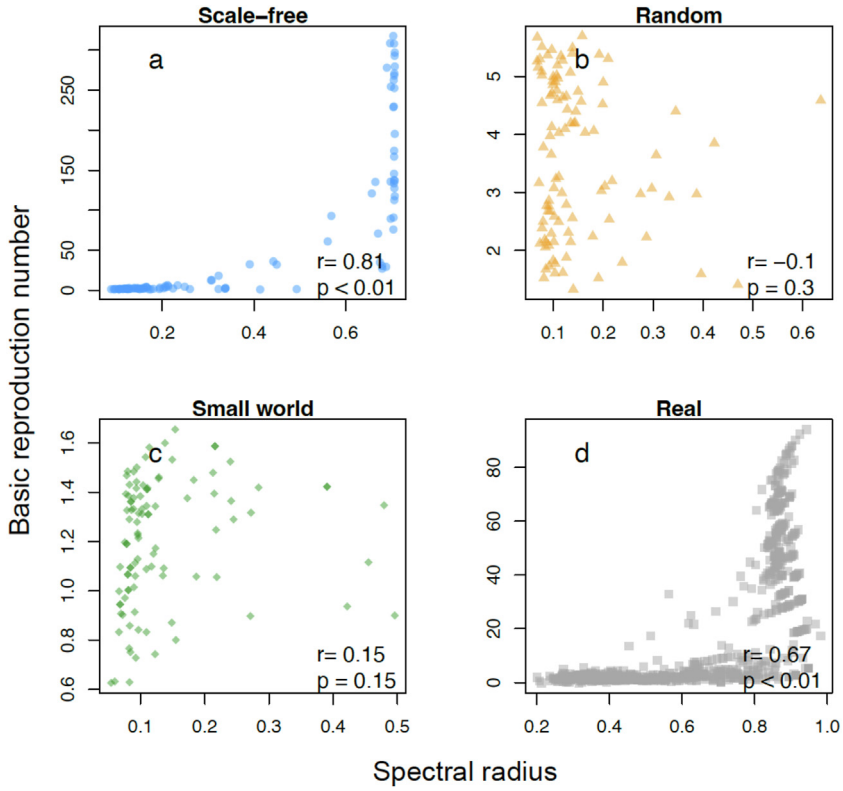

Fig. 4. The relationship between basic reproduction number (R_0) and spectral radius for constructed networks adhering to three different network types (*a*–*c*) and for empirical biological social contact networks (*d*). Each plotted point corresponds to a network, where 100 random networks were generated for each of the network types, and all of the 782 empirical networks were plotted.

and measles (Bharti et al., 2010). Additionally, links between network structure and spectral properties, which have important implications to pathogen spread, have been identified in terms of the number of sub-communities in a network (Chauhan et al., 2009) and difference in network type (e.g. scale-free and small world) (Farkas et al., 2001).

R_0 has received criticisms related to the unreliability, inconsistency in formulation, and misapplication of the measure (Li et al., 2011; Delamater et al., 2019). In contrast, spectral radius is an intrinsic characteristic of a network, there is only one method to calculate it, and no prior knowledge about a disease is required for its calculation. Spectral radius might be particularly valuable in situations in which little is known about a disease or in assessing the general vulnerability of a network. The potential we recognize in spectral radius as an epidemic susceptibility indicator has been reflected in previous studies, with one publication even referring to spectral radius as the ideal "vulnerability measure" of a network (Tong et al., 2010) and others developing strategies for reducing spectral radius to control epidemic size (Saha et al., 2015; Tong et al., 2012; Van Mieghem et al., 2011).

Epidemics present a clear global threat, and understanding how network topological properties translate to dynamic epidemic processes is key in predicting and preventing epidemics in natural systems. Our findings may have implications for epidemic management policy. R_0 has been used as an indicator of epidemic outbreak in many prior studies (Guerra et al., 2017; Lim et al., 2016; Towers et al., 2016) and spectral radius, although less often utilized, has also been used as an indicator (Liu & Van Mieghem, 2016, 2018; Socievole et al., 2016). Social contact networks differ in the size of epidemics that they can produce in both simulated and empirical networks, suggesting an inherent link between static network structure and dynamic infection processes. One future direction of this research is looking at changes in spectral radius and R_0 due to rerouted links. Changing links may have a greater effect on spectral radius than R_0, which might better reflect infection spread.

The spectral radius of a social contact network offers a way to design or modify social networks to reduce the overall size of epidemics. Paired with basic reproduction number, these two epidemic susceptibility indicators may provide a more comprehensive understanding of infection spread throughout a network. Translating this to transportation, computer, and other unipartite networks of importance, spectral graph theory may be useful in designing robust networks in the face of perturbations as well as assessing the vulnerability of existing networks.

Author contributions

JAM and TAD designed the experiment, performed the analyses, and collaboratively wrote the manuscript. Both authors approved the final manuscript.

Data accessibility

R code is available on figshare at https://doi.org/10.6084/m9.figshare.12059526.v3.

CRediT authorship contribution statement

Jae McKee: Conceptualization, Investigation, Methodology, Visualization, Writing – original draft. **Tad Dallas:** Conceptualization, Formal analysis, Funding acquisition, Investigation, Methodology, Project administration, Visualization, Writing – review & editing.

Declaration of competing interest

The authors declare no competing interests.

Acknowledgments

This work has been supported by the U.S. National Science Foundation RAPID grant (NSF-DEB-2031196).

Appendix A. Supplementary data

Supplementary data to this article can be found online at https://doi.org/10.1016/j.idm.2023.12.008.

References

Akbaş, M.İ., Brust, M. R., Turgut, D., & Ribeiro, C. H. (2015). A preferential attachment model for primate social networks. *Computer Networks, 76*, 207–226.
Barabási, A.-L., & Albert, R. (1999). Emergence of scaling in random networks. *Science, 286*(5439), 509–512.
Barabási, A.-L., & Bonabeau, E. (2003). Scale-free networks. *Scientific American, 288*(5), 60–69.
Barber, M. J. (2007). Modularity and community detection in bipartite networks. *Physical Review E, 76*(6).
Bharti, N., Djibo, A., Ferrari, M. J., Grais, R., Tatem, A., McCabe, C., Bjornstad, O. N., & Grenfell, B. T. (2010). Measles hotspots and epidemiological connectivity. *Epidemiology and Infection, 138*(9), 1308–1316.
Britton, T. (2019). *Epidemic models on social networks—with inference. arXiv preprint arXiv:1908.05517.*

Campbell, E., & Salathé, M. (2013). Complex social contagion makes networks more vulnerable to disease outbreaks. *Scientific Reports, 3*, 1905.
Castellano, C., & Pastor-Satorras, R. (2019). Thresholds for epidemic spreading in networks. *Physical Review Letters, 105*(21), 218701-1–218701-4.
Chauhan, S., Girvan, M., & Ott, E. (2009). Spectral properties of networks with community structure. *Physical Review E, 80*(5), Article 056114.
Craft, M. E. (2015). Infectious disease transmission and contact networks in wildlife and livestock. *Philosophical Transactions of the Royal Society B: Biological Sciences, 370*(1669), Article 20140107.
Craft, M. E., Volz, E., Packer, C., & Meyers, L. A. (2011). Disease transmission in territorial populations: The small-world network of serengeti lions. *Journal of the Royal Society Interface, 8*(59), 776–786.
Danon, L., Ford, A. P., House, T., Jewell, C. P., Keeling, M. J., Roberts, G. O., Ross, J. V., & Vernon, M. C. (2011). Networks and the epidemiology of infectious disease. *Interdisciplinary perspectives on infectious diseases*, 2011.
Delamater, P. L., Street, E. J., Leslie, T. F., Yang, Y. T., & Jacobsen, K. H. (2019). Complexity of the basic reproduction number (r0). *Emerging Infectious Diseases, 25*(1), 1.
Diekmann, O., Heesterbeek, J. A. P., & Metz, J. A. (1990). On the definition and the computation of the basic reproduction ratio r 0 in models for infectious diseases in heterogeneous populations. *Journal of Mathematical Biology, 28*(4), 365–382.
Dietz, K. (1993). The estimation of the basic reproduction number for infectious diseases. *Statistical Methods in Medical Research, 2*(1), 23–41.
Dinh, T. N., & Thai, M. T. (2013). Community detection in scale-free networks: Approximation algorithms for maximizing modularity. *IEEE Journal on Selected Areas in Communications, 31*(6), 997–1006.
Eames, K. T., & Keeling, M. J. (2003). Contact tracing and disease control. *Proceedings of the Royal Society of London. Series B: Biological Sciences, 270*(1533), 2565–2571.
Erdös, P., & Rényi, A. (1959). On random graphs i. *Publ. Math. Debrecen, 6*(290–297), 18.
Farkas, I. J., Derényi, I., Barabási, A.-L., & Vicsek, T. (2001). Spectra of "real-world" graphs: Beyond the semicircle law. *Physical Review E, 64*(2), Article 026704.
Ganesh, A., Massoulié, L., & Towsley, D. (2005). The effect of network topology on the spread of epidemics. In *Proceedings IEEE 24th annual joint conference of the IEEE computer and communications societies* (Vol. 2, pp. 1455–1466). IEEE.
Goltsev, A. V., Dorogovtsev, S. N., Oliveira, J. G., & Mendes, J. F. (2012). Localization and spreading of diseases in complex networks. *Physical Review Letters, 109*(12), Article 128702.
Griffin, J. T. (2015). The interaction between seasonality and pulsed interventions against malaria in their effects on the reproduction number. *PLoS Computational Biology, 11*(1), Article e1004057.
Grilli, J., Rogers, T., & Allesina, S. (2016). Modularity and stability in ecological communities. *Nature Communications, 7*(1), 1–10.
Guerra, F. M., Bolotin, S., Lim, G., Heffernan, J., Deeks, S. L., Li, Y., & Crowcroft, N. S. (2017). The basic reproduction number (r0) of measles: A systematic review. *The Lancet Infectious Diseases, 17*(12).
Heesterbeek, J., & Dietz, K. (1996). The concept of ro in epidemic theory. *Statistica Neerlandica, 50*(1), 89–110.
Heffernan, J. M., Smith, R. J., & Wahl, L. M. (2005). Perspectives on the basic reproductive ratio. *Journal of the Royal Society Interface, 2*(4), 281–293.
Herrera, J. L., Srinivasan, R., Brownstein, J. S., Galvani, A. P., & Meyers, L. A. (2016). Disease surveillance on complex social networks. *PLoS Computational Biology, 12*(7).
Holme, P., & Masuda, N. (2015). The basic reproduction number as a predictor for epidemic outbreaks in temporal networks. *PLoS One, 10*(3), Article e0120567.
Huerta, R., & Tsimring, L. S. (2002). Contact tracing and epidemics control in social networks. *Physical Review E, 66*(5), Article 056115.
Jeger, M. (2004). Analysis of disease progress as a basis for evaluating disease management practices. *Annual Review of Phytopathology, 42*, 61–82.
Keeling, M. J. (1999). The effects of local spatial structure on epidemiological invasions. *Proceedings of the Royal Society of London. Series B: Biological Sciences, 266*(1421), 859–867.
Keeling, M. J., & Eames, K. T. (2005). Networks and epidemic models. *Journal of the Royal Society Interface, 2*(4), 295–307.
Kiskowski, M., & Chowell, G. (2016). Modeling household and community transmission of ebola virus disease: Epidemic growth, spatial dynamics and insights for epidemic control. *Virulence, 7*(2), 163–173.
Kossinets, G., & Watts, D. J. (2006). Empirical analysis of an evolving social network. *Science, 311*(5757), 88–99.
Latora, V., & Marchiori, M. (2002). Is the boston subway a small-world network? *Physica A: Statistical Mechanics and Its Applications, 314*(1–4), 109–113.
Li, W., & Cai, X. (2004). Statistical analysis of airport network of China. *Physical Review E, 69*(4), Article 046106.
Liljeros, F., Edling, C. R., Amaral, L. A. N., Stanley, H. E., & Åberg, Y. (2001). The web of human sexual contacts. *Nature, 411*(6840), 907–908.
Lim, C., Jiang, L., Ma, S., James, L., & Ang, L. (2016). Basic reproduction number of coxsackievirus type a6 and a16 and enterovirus 71: Estimates from outbreaks of hand, foot and mouth disease in singapore, a tropical city-state. *Epidemiology and Infection, 144*(5), 1028–1034.
Liu, Q., Ajelli, M., Aleta, A., Merler, S., Moreno, Y., & Vespignani, A. (2018). Measurability of the epidemic reproduction number in data-driven contact networks. *Proceedings of the National Academy of Sciences, 115*(50), 12680–12685.
Liu, Q., & Van Mieghem, P. (2016). Die-out probability in sis epidemic processes on networks. In *International workshop on complex networks and their applications* (pp. 511–521). Springer.
Liu, Q., & Van Mieghem, P. (2018). Burst of virus infection and a possibly largest epidemic threshold of non-markovian susceptible-infected-susceptible processes on networks. *Physical Review E, 97*(2), Article 022309.
Milgram, S. (1967). The small world problem. *Psychology Today, 2*(1), 60–67.
Newman, M. E., et al. (2003). Random graphs as models of networks. *Handbook of graphs and networks, 1*, 35–68.
Pastor-Satorras, R., Castellano, C., Van Mieghem, P., & Vespignani, A. (2015). Epidemic processes in complex networks. *Reviews of Modern Physics, 87*(3), 925.
Rodrigues, H. S., Monteiro, M. T. T., & Torres, D. F. (2016). Seasonality effects on dengue: Basic reproduction number, sensitivity analysis and optimal control. *Mathematical Methods in the Applied Sciences, 39*(16), 4671–4679.
Saha, S., Adiga, A., Prakash, B. A., & Vullikanti, A. K. S. (2015). Approximation algorithms for reducing the spectral radius to control epidemic spread. In *Proceedings of the 2015 SIAM international conference on data mining* (pp. 568–576). SIAM.
Sah, P., Mendez, J. D., & Bansal, S. (2019). A multi-species repository of social networks. *Scientific Data, 6*(1), 44.
Salathé, M., Kazandjieva, M., Lee, J. W., Levis, P., Feldman, M. W., & Jones, J. H. (2010). A high-resolution human contact network for infectious disease transmission. *Proceedings of the National Academy of Sciences, 107*(51), 22020–22025.
Sarkar, C., & Jalan, S. (2018). Spectral properties of complex networks. *Chaos: An Interdisciplinary Journal of Nonlinear Science, 28*(10), Article 102101.
Sen, P., Dasgupta, S., Chatterjee, A., Sreeram, P., Mukherjee, G., & Manna, S. (2003). Small-world properties of the indian railway network. *Physical Review E, 67*(3), Article 036106.
Shirely, M., & Rushton, S. (2005). The impacts of network topology on disease spread. *Ecological Complexity, 2*(3), 287–299.
Silk, M. J., Croft, D. P., Delahay, R. J., Hodgson, D. J., Boots, M., Weber, N., & McDonald, R. A. (2017). Using social network measures in wildlife disease ecology, epidemiology, and management. *BioScience, 67*(3), 245–257.
Small, M., Walker, D. M., & Tse, C. K. (2007). Scale-free distribution of avian influenza outbreaks. *Physical Review Letters, 99*(18), Article 188702.
Smith, D. L., McKenzie, F. E., Snow, R. W., & Hay, S. I. (2007). Revisiting the basic reproductive number for malaria and its implications for malaria control. *PLoS Biology, 5*(3), 1–12.
Socievole, A., Rango, F. D., Scoglio, C., & Mieghem, P. V. (2016). Assessing network robustness under sis epidemics: The relationship between epidemic threshold and viral conductance. *Computer Networks, 103*, 196–206.
Stevanovic, D. (2014). *Spectral radius of graphs*. Academic Press.
Suleman, M., & Riaz, S. (2017). Unconditionally stable numerical scheme to study the dynamics of hepatitis b disease. *Punjab University Journal of Mathematics, 49*, 99–118.

Supriatna, A. K. (2009). *Estimating the basic reproduction number of dengue transmission during 2002-2007 outbreaks in bandung, Indonesia*. WHO Regional Office for South-East Asia.
Tatem, A. J., Hemelaar, J., Gray, R. R., & Salemi, M. (2012). Spatial accessibility and the spread of hiv-1 subtypes and recombinants. *Aids, 26*(18), 2351–2360.
Tong, H., Prakash, B. A., Eliassi-Rad, T., Faloutsos, M., & Faloutsos, C. (2012). Gelling, and melting, large graphs by edge manipulation. In *Proceedings of the 21st ACM international conference on Information and knowledge management* (pp. 245–254).
Tong, H., Prakash, B. A., Tsourakakis, C., Eliassi-Rad, T., Faloutsos, C., & Chau, D. H. (2010). On the vulnerability of large graphs. In *2010 IEEE international conference on data mining* (pp. 1091–1096). IEEE.
Towers, S., Brauer, F., Castillo-Chavez, C., Falconar, A. K., Mubayi, A., & Romero-Vivas, C. M. (2016). Estimate of the reproduction number of the 2015 zika virus outbreak in barranquilla, Colombia, and estimation of the relative role of sexual transmission. *Epidemics, 17*, 50–55.
Trapman, P., Ball, F., Dhersin, J., Tran, V. C., Wallinga, J., and Britton, T. Inferring R 0 in emerging epidemics—the effect of common population structure is small Journal of The Royal Society Interface, 13(121): 20160288.
Valdano, E., Ferreri, L., Poletto, C., & Colizza, V. (2015). Analytical computation of the epidemic threshold on temporal networks. *Physical Review X, 5*(2), Article 021005.
Van Kerkhove, M. D., Bento, A. I., Mills, H. L., Ferguson, N. M., & Donnelly, C. A. (2015). A review of epidemiological parameters from ebola outbreaks to inform early public health decision-making. *Scientific Data, 2*, Article 150019.
Van Mieghem, P., Stevanović, D., Kuipers, F., Li, C., Van De Bovenkamp, R., Liu, D., & Wang, H. (2011). Decreasing the spectral radius of a graph by link removals. *Physical Review E, 84*(1), Article 016101.
Volz, E., & Meyers, L. A. (2009). Epidemic thresholds in dynamic contact networks. *Journal of the Royal Society Interface, 6*(32), 233–241.
Wang, Y., Chakrabarti, D., Wang, C., & Faloutsos, C. (2003). Epidemic spreading in real networks: An eigenvalue viewpoint. In *22nd international symposium on reliable distributed systems* (pp. 25–34). IEEE.
Watts, D. J., & Strogatz, S. H. (1998). Collective dynamics of 'small-world'networks. *Nature, 393*(6684), 440.
Wearing, H. J., Rohani, P., & Keeling, M. J. (2005). Appropriate models for the management of infectious diseases. *PLoS Medicine, 2*(7).
Youssef, M., & Scoglio, C. (2011). An individual-based approach to sir epidemics in contact networks. *Journal of Theoretical Biology, 283*(1), 136–144.